SAND 2000-0154J

Reductive precipitation of metals photosensitized by tin protoporphyrin

A. Abdelouas[†], W. L. Gong[†], W. Lutze[‡], J. A. Shelnutt[§,*]

[†] Center for Radioactive Waste Management (CeRaM), The University of New Mexico, 1001 University Blvd., SE, Albuquerque, NM 87106;
[‡] Department of Chemical and Nuclear Engineering, The University of New Mexico, Farris Engineering Center, Albuquerque, NM 87131;
[§] Biomolecular Materials and Interfaces Department, Sandia National Laboratories, Albuquerque, NM 87185-1349, and Department of Chemistry, The University of New Mexico, Albuquerque, NM 87131.

* Sandia is a multiprogram laboratory operated by Sandia Corp., a Lockheed Martin Co., for the United States Department of Energy under Contract DE-AC04-94AL85000.

Introduction

Metalloporphyrin complexes exhibit an wide range of biological functions in proteins. For instance, the iron porphyrin (heme) in cytochrome c_3, a well studied protein found in iron-reducing bacteria (*Shewanella frigidamarina*) or sulfate-reducing bacteria (*e.g.*, *Desulfovibrio desulfuricans*),[21,22] is likely involved in electron transport. Recently, it was recognized that cytochrome c_3 also catalyzes the non-biological reduction of metals such as U, Cr and Se. Thus, cytochrome c_3 was suggested as a protein useful for remediation of contaminated water via reductive precipitation of metals. Furthermore, we recently found that selenium precipitated by cytochrome c_3 as nanoparticles with an average size of 40 nm.[22] Based on these results with the native protein, it was thought that some porphyrins, *e.g.*, tin porphyrins, *without the surrounding protein* might also be used to mediate reduction reactions for metals. Using tin porphyrins to remove metals from solutions and, perhaps, to form metal nanoparticles is attractive because it uses sun light as a source of energy to produce the required strongly reducing species.[2,7]

Photoinduced redox reactions of a three-component system containing a photosensitizer, an electron donor, and an electron acceptor have been studied by several authors.[1-5] Metalloporphyrins are well studied photosensitizers for the reduction of various acceptor, usually methylviologen.[5] For example, photoreduced tin porphyrins act as strong reductants in solution, in micelles, and at water-organic solvent interfaces, upon excitation by visible light and reduction

by an electron donor such as a tertiary amine.[2,4-6]

Shelnutt[2,7] studied the ternary system comprised of Sn(IV) protoporphyrin IX (SnPP), triethanolamine (TEA), and methylviologen (MV^{2+}), where SnPP is the photosensitizer, TEA is the electron donor, and MV^{2+} is the electron acceptor. The photoinduced oxidation-reduction reaction is illustrated in Figure 1. Irradiation of SnPP by visible light leads to excitation of the porphyrin to its lowest-lying triplet •-• state (SnPP*). Because the redox potential of the couple SnPP*/SnPP (+1.1 V) is higher than that of TEA/TEA_{ox} (+0.82 V), excited SnPP* accepts an electron from TEA resulting in the radical porphyrin anion (Figure 1). The low redox potential of the $SnPP^{\bullet-}/SnPP$ couple (-0.66 V) allows the reduction of MV^{2+} to MV^{+} (MV^{2+}/MV^{+}; -0.45 V).[5] The quantum yield for the reaction is near 0.8.

The objective of this work was to investigate the possibility of reduction of a variety of metals by SnPP and light. Two types of metals were investigated: (1) U, Hg and Cu, which are common contaminants in wastewater and groundwater,[8-11] and (2) Au, Ag and Pt, which are precious metals. Thermodynamically, all these metals can be reduced by SnPP.[12] Reduction reactions of the metals are listed in equations (1) to (6). For the first group of metals, their precipitation may be an interesting technique to remediate contaminated waters. For the second group, their concentration from aqueous solutions is a useful goal and is of interest in metal refining and materials processing.

$$2SnPP^{-} + UO_2(NO_3)_2.6H_2O = 2SnPP + UO_2 + 2NO_3^{-} + 6H_2O \qquad (1)$$

$$2SnPP^{-} + HgCl_2 = 2SnPP + Hg^0 + 2Cl^{-} \qquad (2)$$

$$2SnPP^{-} + CuCl_2.2H_2O = 2SnPP + Cu^0 + 2Cl^{-} + 2H_2O \qquad (3)$$

$$2SnPP^{-} + Ag(NO_3)_2 = 2SnPP + Ag^0 + 2NO_3^{-} \qquad (4)$$

$$3SnPP^{-} + HAuCl_4.xH_2O = 3SnPP + Au^0 + 4Cl^{-} + H^{+} + xH_2O \qquad (5)$$

$$4SnPP^{-} + H_2PtCl_6.6H_2O = 4SnPP + Pt^0 + 6Cl^{-} + 2H^{+} + 6H_2O \qquad (6)$$

Experimental section

Stock 10-mM solutions of each of the metals were prepared by dissolving their respective salts in deionized water. SnPP was obtained from Porphyrin Products and used without further purification. In aqueous solution, SnPP exists as the dihydroxyl complex. TEA and the metal salts were of the highest purity commercially available.

For each experiment, the final concentration of the different components were: [metal] = 10^{-2} M; [SnPP] = 10^{-6} M; [TEA] = 4×10^{-1} M. Experiments with MV^{2+} as the electron acceptor show that the reduction reaction, as demonstrated by the blue color of MV^{+}, took place under sunlight, although it was faster under an artificial tungsten light. Oxygenation of the solution led to the reoxidation of MV^{+} to MV^{2+} although it did not affect the stability of SnPP. In fact, following oxygenation, evidenced by the loss of blue color due to oxidation of MV^{+} to MV^{2+}, the reverse reduction reaction occurred in light and this reduction/oxidation cycle was repeated several times. Precipitation of metals was very fast (a few minutes) for certain metals (Ag, Hg), but took from a few hours to a few days for the rest of metals.

A few drops of the metal suspension were deposited onto a carbon-coated grid and rinsed with de-ionized water to remove soluble salts. The grid was placed into a Jeol JEM-2010 transmission electron microscope (TEM), equipped with an Oxford Link ISIS energy dispersive spectrometry (EDS) system. The microscope was operated at 200 keV. The precipitate was analyzed for chemical composition and morphology. Crystal structure information was obtained using selected area electron diffraction (SAED).

Results and Discussion

Reduction of U^{VI}, Hg^{II} and Cu^{II}. In the experiments with uranium, the appearance of a black precipitate was correlated with the decrease in the intensity of the yellow color of uranyl ion. The particles remained in suspension for several days. TEM results with uranium are given in Figure 2. Figure 2a shows uranium-rich particles along with their electron diffraction pattern. The particles are very small with an average diameter of 10 nm. The *d*-spacings (0.315, 0.274, 0.195, 0.164, 0.127 and 0.112 nm) of particles closely match those of uraninite (UO_2). EDS measurements showed the particles consisted of U and O (Figure 2b). In the experiment with Hg, a gray precipitate appeared after only a few minutes and deposited onto the bottom of the vial within the hour. Figure 3a is a TEM image of the Hg-rich particles exhibiting a spherical shape. The particles evaporated under the electron beam, a characteristic of liquid mercury. EDS measurements confirmed the presence of Hg^0 (Figure 3b). It was not possible to obtain

SAED data. In the experiment with Cu, it took several days for a reddish coating to appear on the glass wall. TEM results with Cu given in Figure 4 show the morphology of the Cu-rich particles. These particles, with an average diameter of few microns, are aggregates of small particles (100 nm in diameter). These particles are pure Cu with traces of oxygen, which may indicate a slight oxidation of the surface of Cu (Figure 4b). Attempts to obtain SAED data failed because the particles are too thick for the electron beam to penetrate. However, the red color of the precipitate, together with their composition, suggests the particles are Cu^0.

The solubility of uraninite (2×10^{-8}),[13] Hg^0 (10^{-29}),[14] and Cu^0 (10^{-44})[13] in water at 25•C is very low. Therefore, their precipitation mediated by the tin protoporphyrin could be used to clean up contaminated waters. Following precipitation, these metal phases may be filtered for reuse or disposed of. Reductive precipitation of metals as a tool for water remediation is an active field of research and was recently proposed by several authors.[9,11,15] Using SnPP for water remediation may be an attractive technique because it uses sun light as the source of energy and an inexpensive and safe commonly-used emulsifier for vegetable oil, paraffin and waxes as the electron donor.

Reduction of precious metals Ag^{II}, Au^{III} and Pt^{IV}. Colloidal suspension of Ag-rich particles was obtained only a few minutes after the beginning of the experiment (Figure 5a). A thin silver film also formed on the glass wall. The average size of these spherical particles was less than 20 nm in diameter. SAED data (0.28, 0.235, 0.200, 0.141, 0.119, 0.0985, 0.083 and 0.077 nm) match those of elemental Ag, and EDS measurements showed the presence of Ag. Oxygen was not detected in agreement with the high stability of Ag in aqueous solutions.[12] Experiments with Au showed the appearance of a golden suspension and correlated with the decrease in the intensity of the yellow color of gold chloride complex. A TEM image of the suspension is given in Figure 6a. Most particles are spherical but some of them have a hexagonal morphology characteristic of Au^0. The average size of the particles is less than 20 nm in diameter. The measured *d*-spacings (0.220, 0.189, 0.132, 0.113, 0.109, 0.0967and 0.085 nm) are similar to those of Au^0, and EDS analysis shows the presence of pure Au. In the experiment with Pt, a black precipitate appeared after few days and deposited onto the bottom of the vial. The particles consisted of rods with several microns in length and 300 nm in diameter (Figure 7a). EDS measurements showed the particles consisted of Pt (Figure 7b). We were not able to obtain SAED data because the particles were too thick for the electron beam to penetrate.

Precipitation of precious metals photosensitized by SnPP may be a practical way to extract and concentrate them from oxidizing waters. Furthermore, in the case of Au and Ag, formation of nanoparticles may find application in a variety of fields due to their optical[16-18] and catalytic properties.[19] The present work is the first report on the formation of Au and Ag nanoparticles photomediated by a tin protoporphyrin at room temperature.

Summary and Conclusion

For the first time, we show that redox-sensitive metals, which are highly soluble in the oxidized state can be reduced and precipitated from aqueous solution using tin protoporphyrin and light in the presence of an electron donor. Hg^{2+} and Cu^{2+} were reduced to the metallic state, and U^{6+} precipitated as oxide with very low solubility, suggesting that removal of these metals via reductive photoreduction and precipitation may be an innovative way for wastewater treatment. Ag^{2+} and Au^{2+} were reduced to the metallic state and precipitated as nanoparticles. Finally, using tin porphyrins and light for a variety of purposes involving reactions that require a low redox potential may be a good step toward energy conservation and environmentally benign processing.

References

1. Kalyanasundaram, H.; Kiwi, J.; Grätzel, M. Helv. Chim. Acta 1978, 61, 2720.
2. Shelnutt, J. A. J. Am. Chem. Soc. 1983, 105, 132.
3. Okura, I.; Kita, T.; Aono, S.; Kaji, N. J. Mol. Catal. 1985, 32, 361.
4. Coutinho, P. J. G.; Costa, S. M. B. J. Photochem. Photobiol. A. Chem. 1994, 82, 149.
5. Song, X-Z., Jia, S-L.; Miura, M.; Ma, J-G.; Shelnutt, J. A. J. Photochem. Photobiol. A. Chem. 1998, 113, 233.
6. Wu, G. Z.; Hu, M.; Leung, H. K. J. Photochem. Photobiol. A. Chem. 1991, 62, 141.

7. Shelnutt, J. A. US Patent 4,568,435, 1986.
8. Byrnes-Brower, J.; Ryan, R. L.; Pazirandeh, M. Environ. Sci. Technol. 1997, 31, 2910.
9. Lovley, D. R. J. Ind. Microbiol. 1995, 14, 85.
10. Macaskie, L. E.; Yong, P.; Doyle, T. C.; Roig, M. G.; Diaz, M.; Manzano, T. Biotechnol. Bioeng. 1997, 53, 100.
11. Abdelouas, A.; Lu, Y-M.; Lutze, W.; Nuttall, H. E. J. Contam. Hydrol. 1998, 35, 17.
12. Pourbaix, M. *Atlas of electrochemical equilibria in aqueous solutions.* NACE International, Cebelcor, 1974.
13. Wolery, T. J. *EQ3NR, A computer program for geochemical aqueous speciation-solubility calculations. Theoretical Manual, User's Guide, and Related Documentation, version 7.0.* UCRL-MA-110662-PT-IV, Lawrence Livermore National Laboratory, Livermore, CA.
14. Lide, D. R. *Handbook of Chemistry and Physics.* 71st edition 1990-1991, CR Press, Boston.
15. Tucker M. D.; Barton L. L.; Thomson, B. M. J. Industr. Microbiol. Biotechnol. 1998, 20, 13.
16. Kreibig, U.; Vollmer, M. *Optical Properties of Metal Clusters*; Springer: Berlin 1995.
17. Creighton, J. A.; Eadon, D. J. J. Chem. Soc., Faraday trans. 1991, 87, 3881.
18. Mulvaney, P. Langmuir 1996, 12, 788.
19. Schmid, G. *Clusters and Colloids: From Theory to Application*; VCH: Weinheim 1994.
20. Tsapin, A.I.; Nealson, K. H.; Meyers, T.; Cusanovich, M. A.; Van Beuumen, J.; Crosby, L. D.; Feinberg, B. A.; Zhang, C. (1996). J. Bacteriol. 1996, 178, 6386-6388.
21. Lovley, D. R.; Widman, P. K.; Woodward, J. C.; Phillips, E. J. P. Appl. Environ. Microbiol. 1993, 59, 3572.
22. Abdelouas, A.; Gong, W. L.; Lutze, W.; Shelnutt, J. A. (submitted to Chem. Mater.), 1999.

Figure Captions

Figure 1. The tin porphyrin mediated photocycle for the reduction of metal salts.

Figure 2. (a) Uraninite nanoparticles, electron diffraction pattern and (b) chemical microanalysis spectrum of uraninite. Cu lines are from the grid.

Figure 3. (a) Mercury particles and (b) chemical microanalysis spectrum of Hg^0. Cu lines are from the grid.

Figure 4. (a) Copper particles and (b) chemical microanalysis spectrum of Cu^0.

Figure 5. (a) Silver nanoparticles, electron diffraction pattern and (b) chemical microanalysis spectrum of Ag^0. Cu lines are from the grid.

Figure 6. (a) Gold nanoparticles, electron diffraction pattern and (b) chemical microanalysis spectrum of Au^0. Cu lines are from the grid.

Figure 7. (a) Platinum particles and (b) chemical microanalysis spectrum of Pt^0.

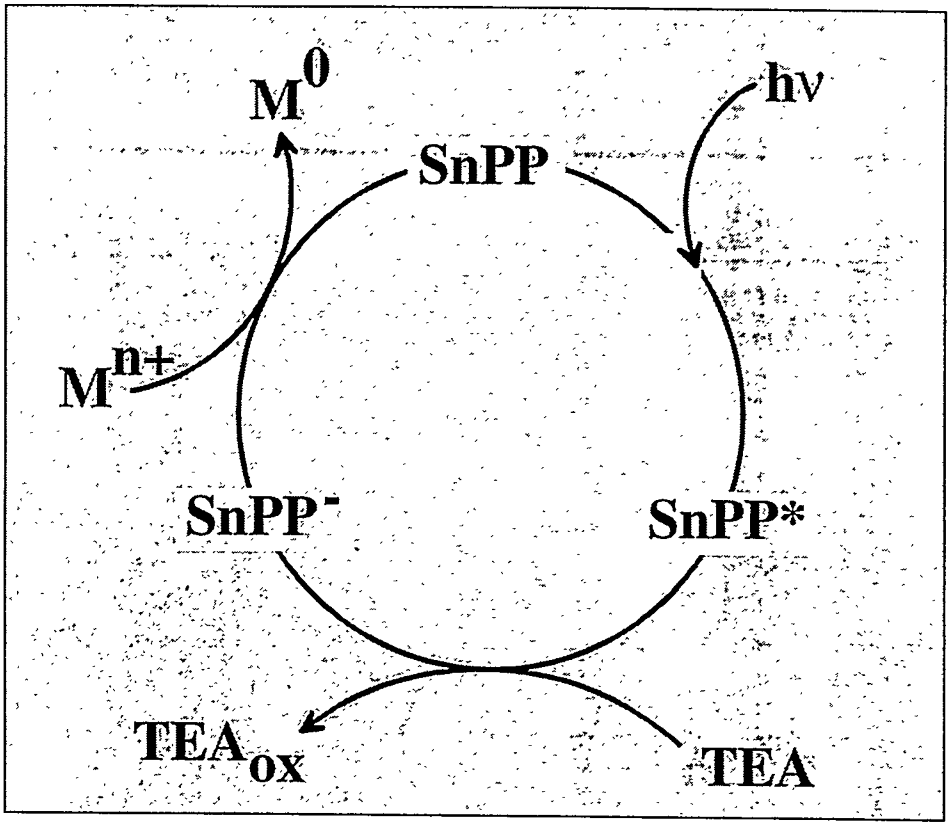

Figure 1.

Fig. 2a

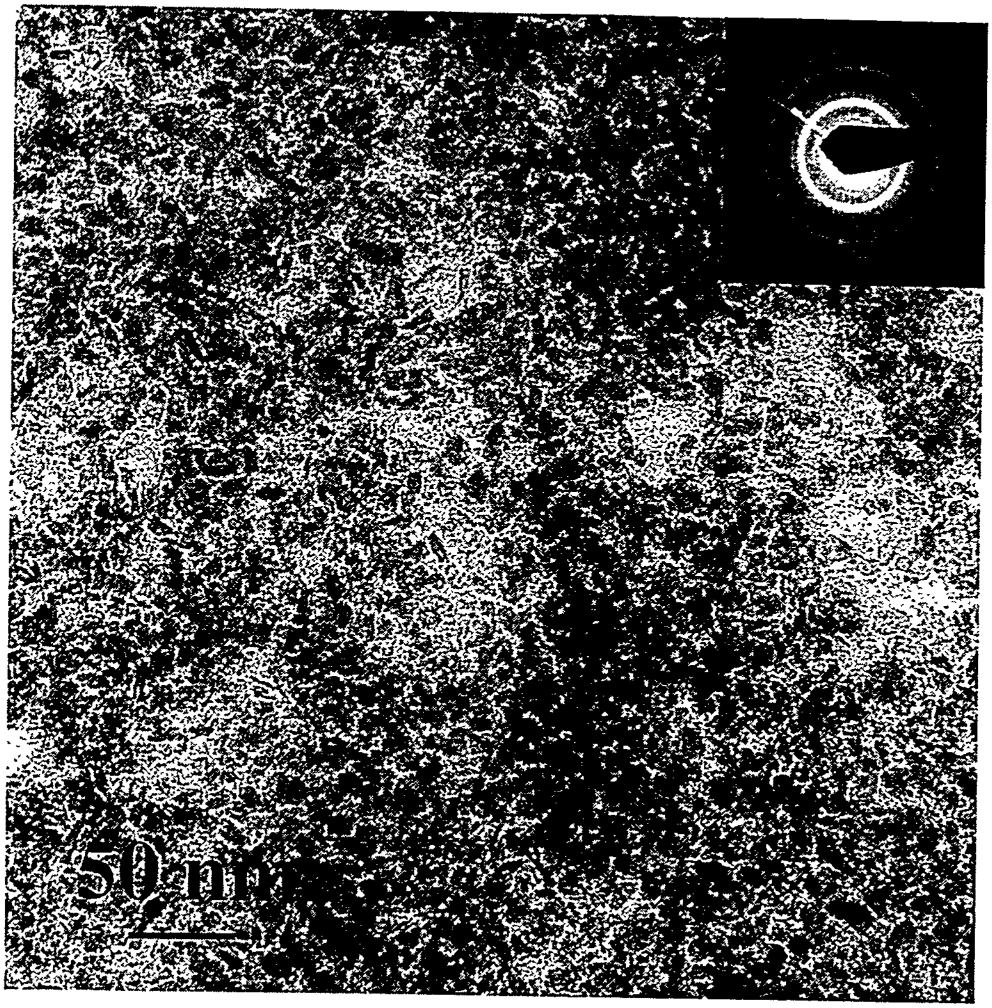

Fig. 2b

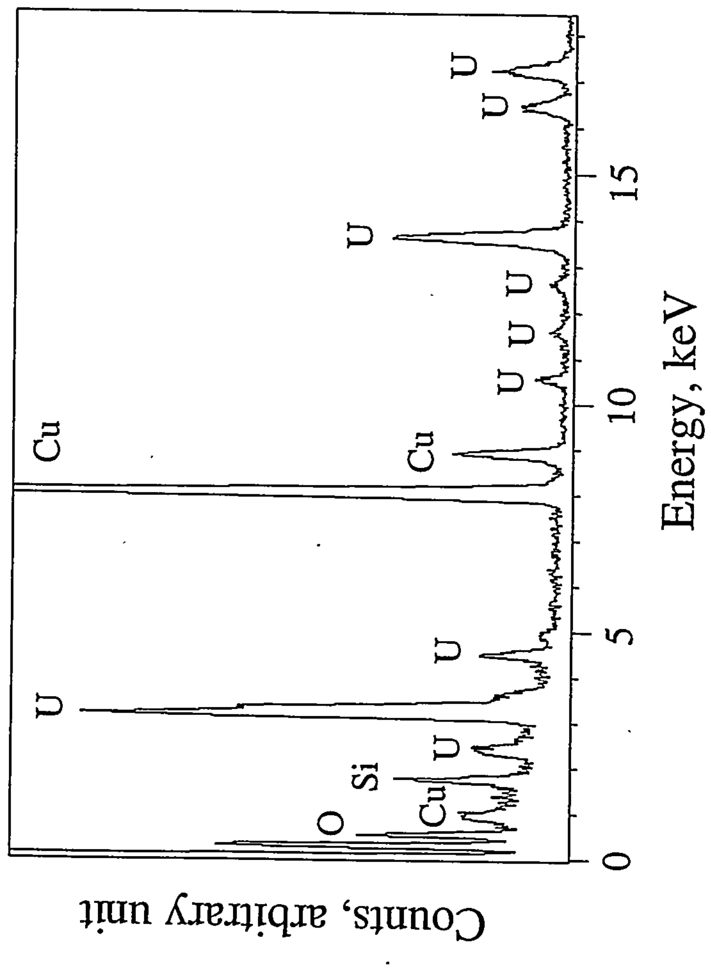

Counts, arbitrary unit
Energy, keV
0
5
10
15
O
Cu
Si
U
U
U
Cu
Cu
U
U
U
U
U
U
U

Fig.3a

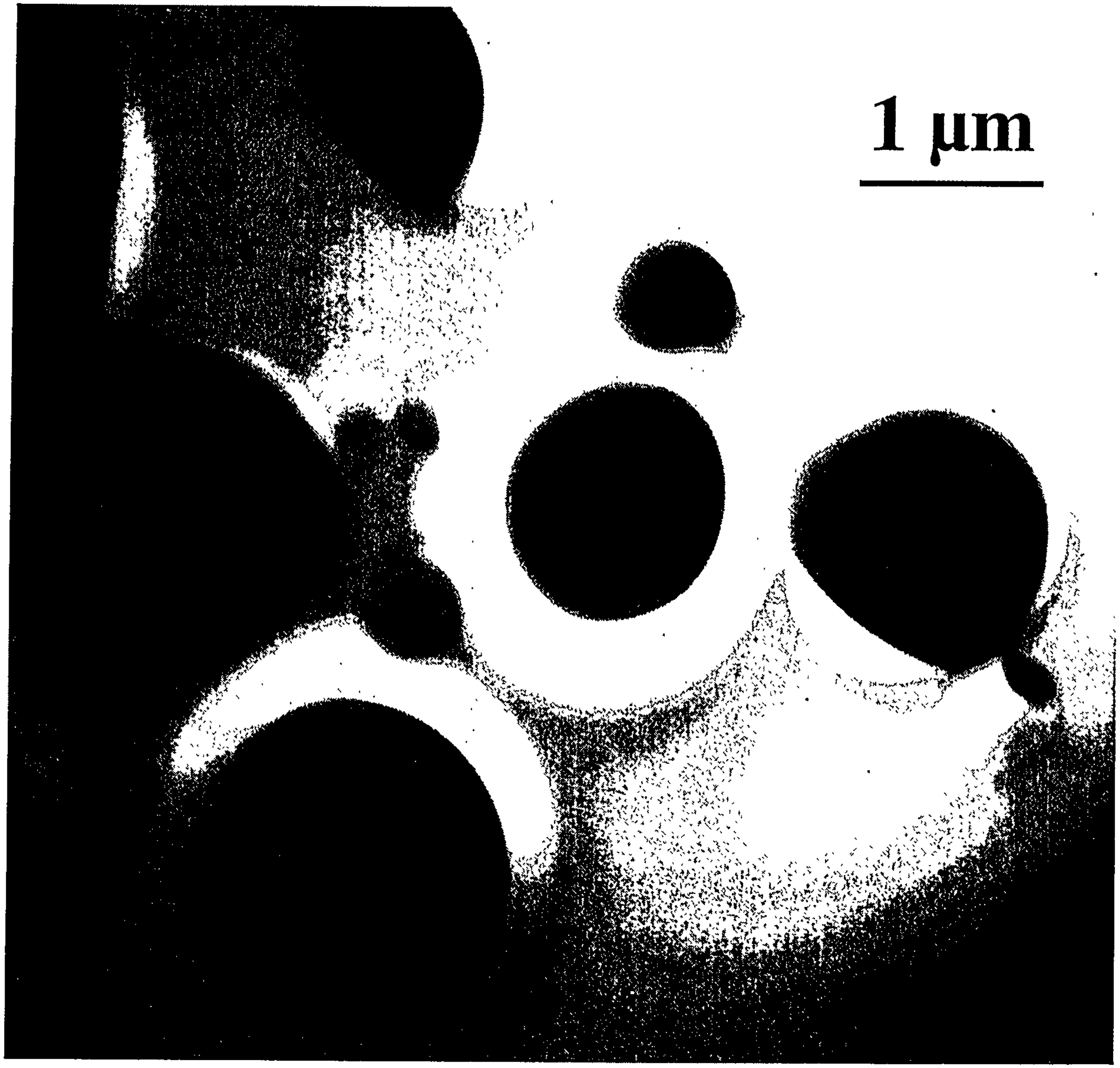

Fig. 3b

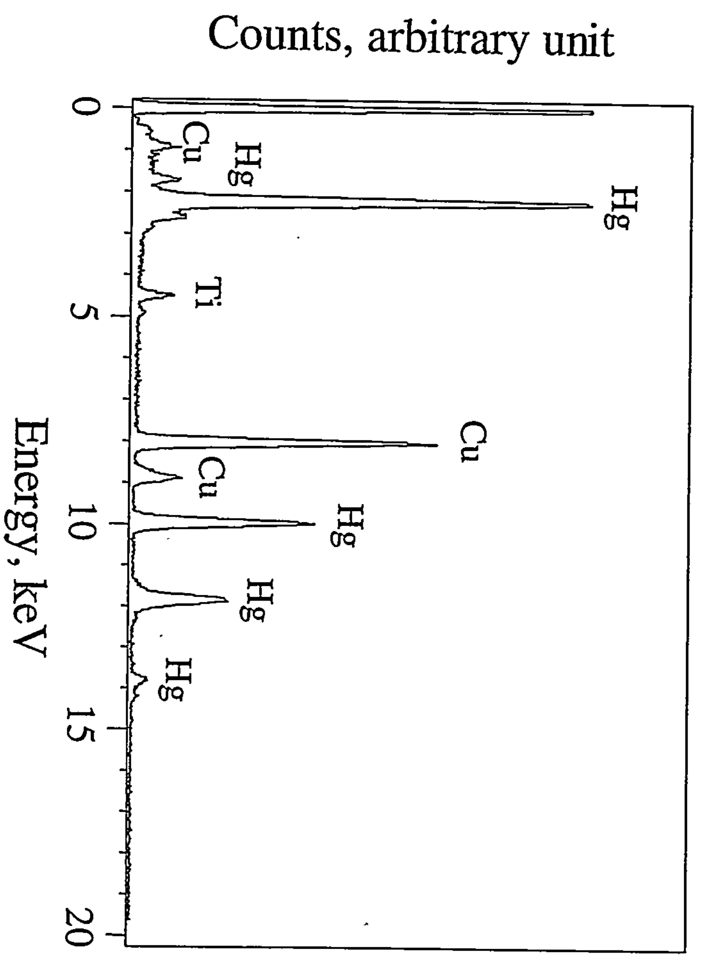
Counts, arbitrary unit
Energy, keV
0
5
10
15
20
Cu
Hg
Hg
Ti
Cu
Cu
Hg
Hg
Hg

Fig.4a

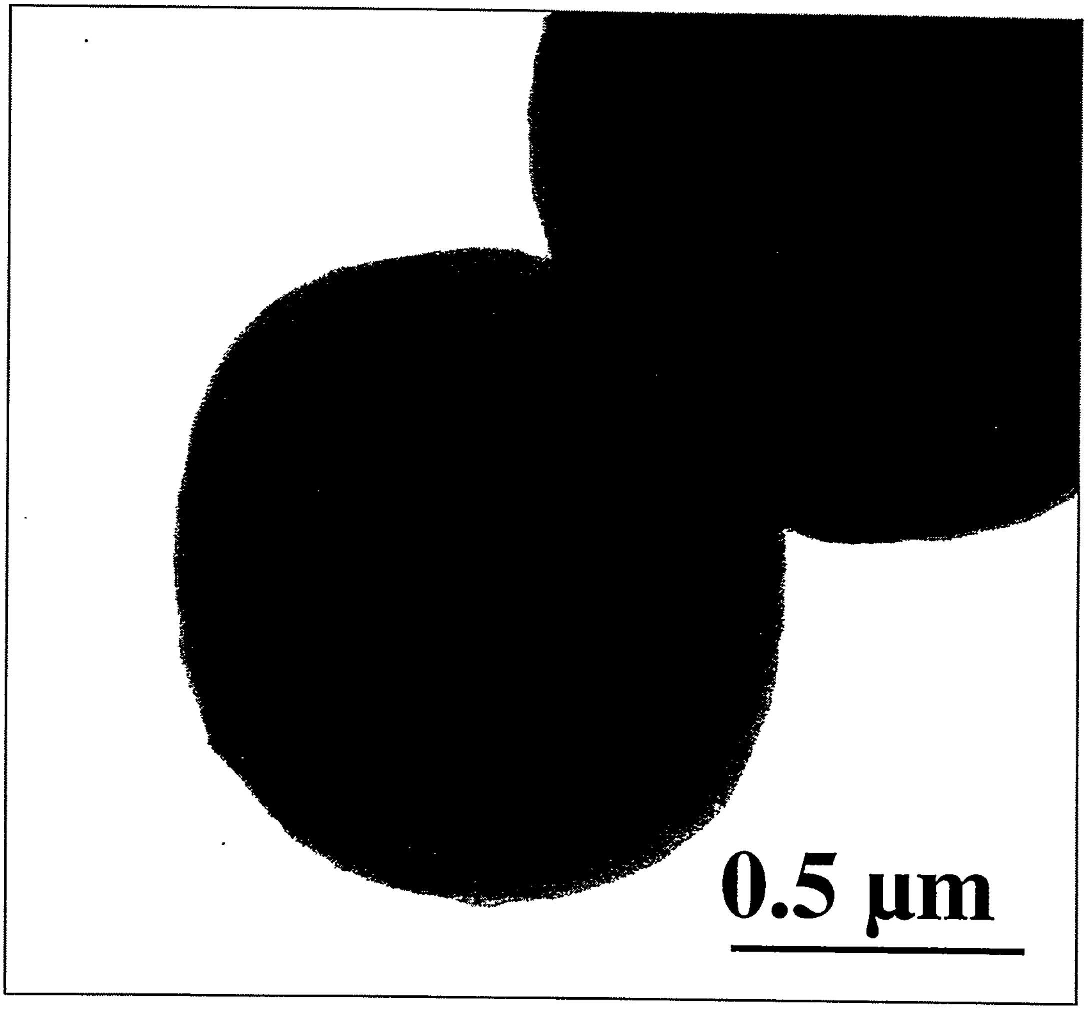

Fig.4b

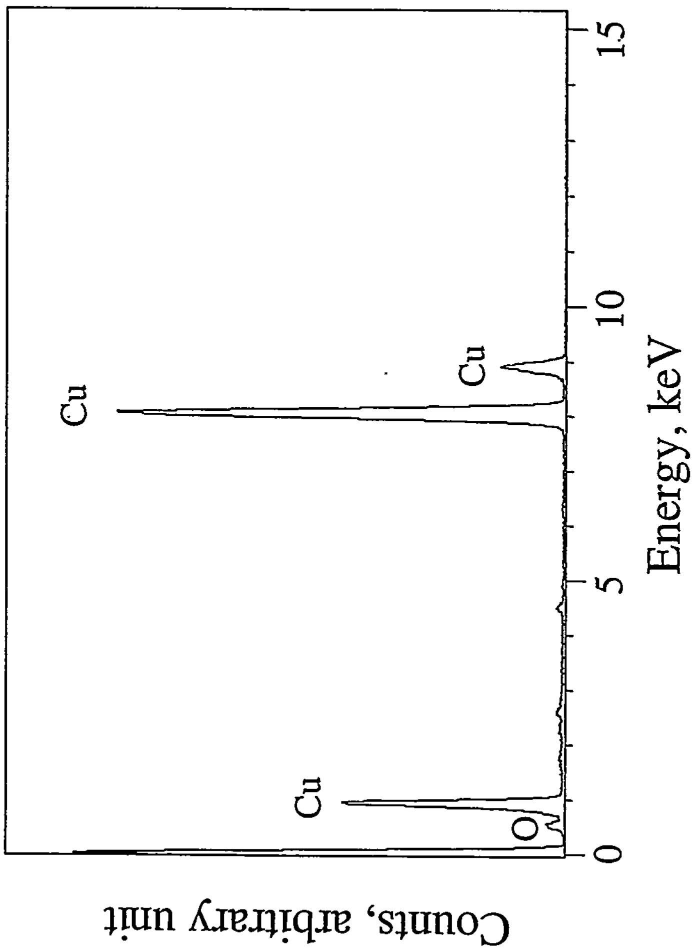

Fig. 5a

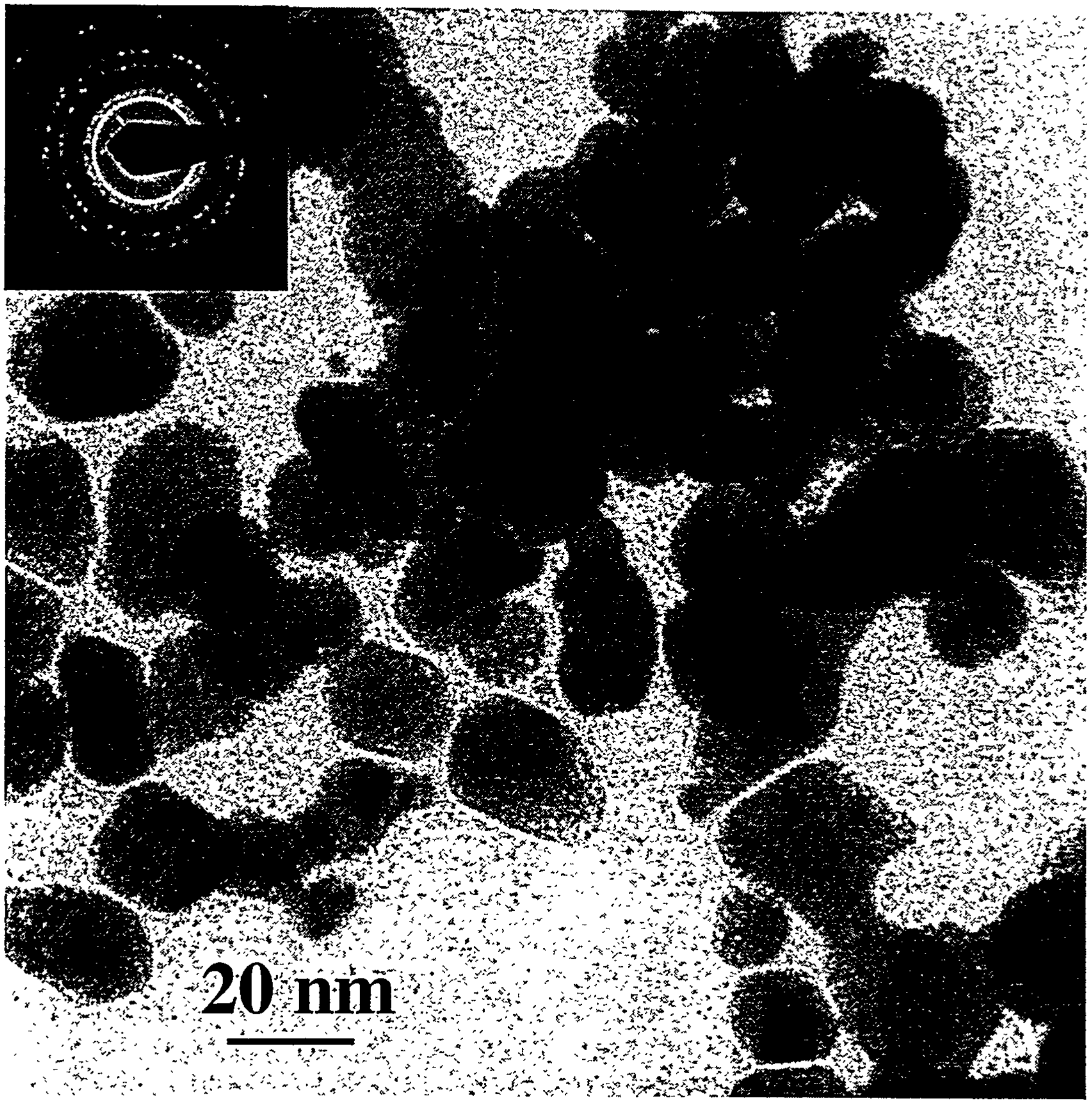

Fig. 5b

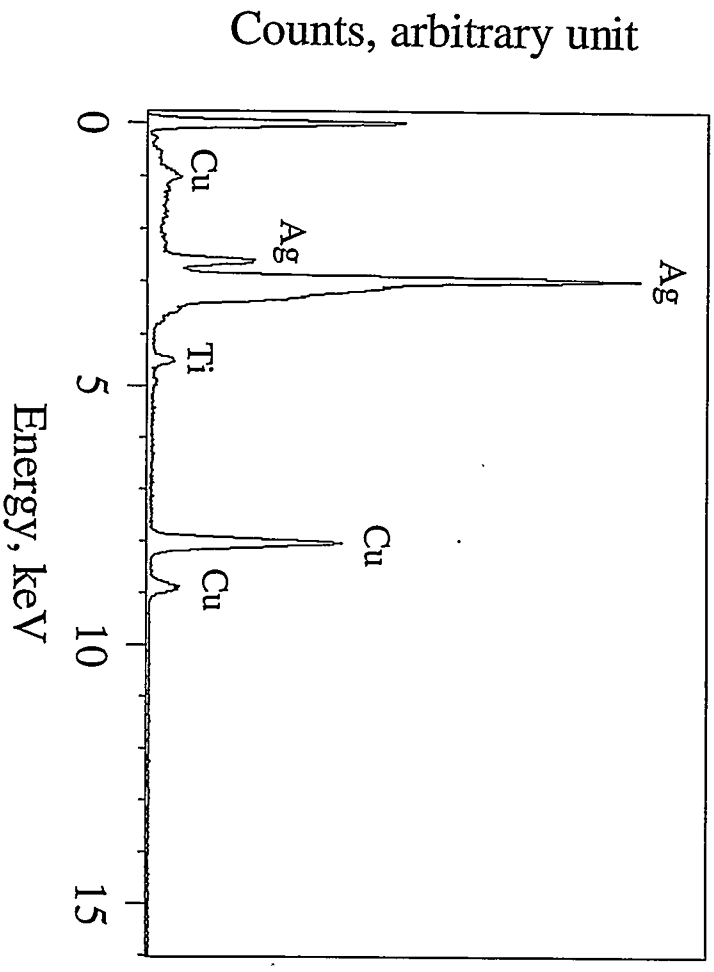

Fig. 6a

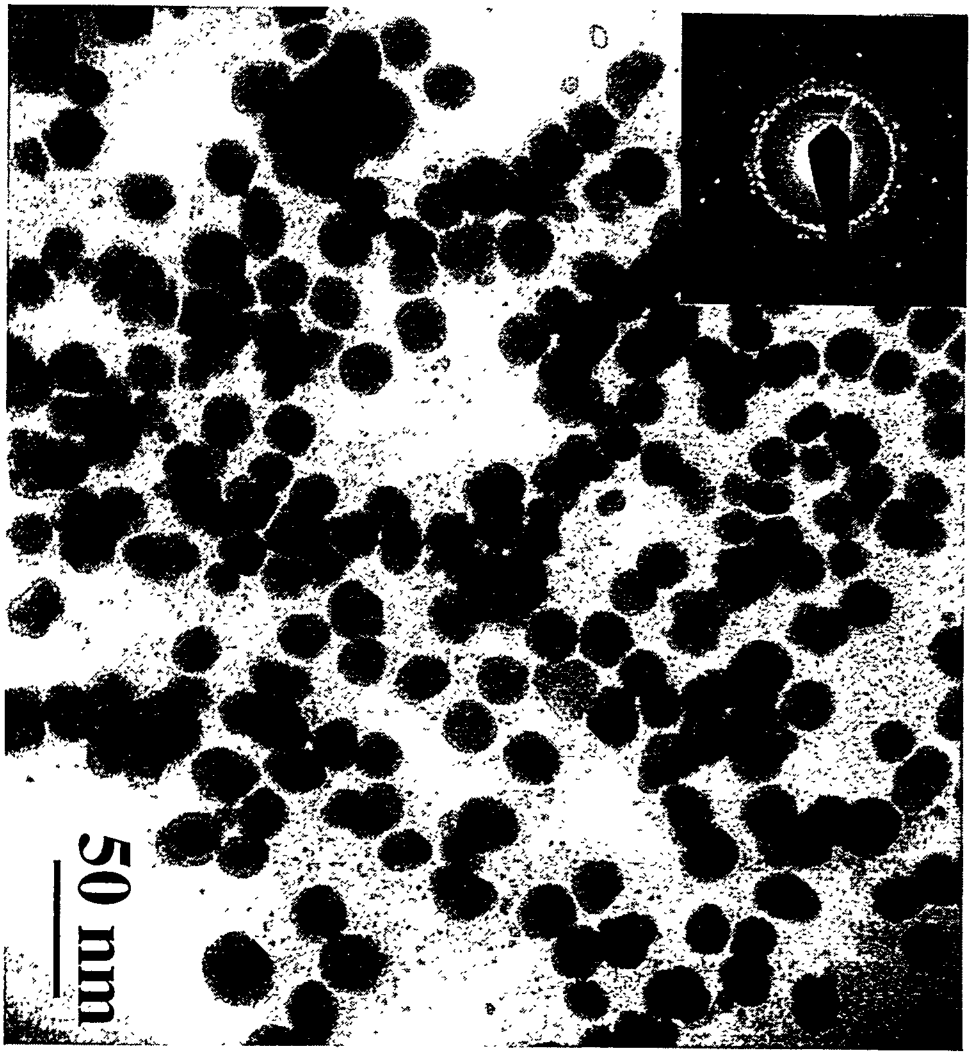

Fig. 6b

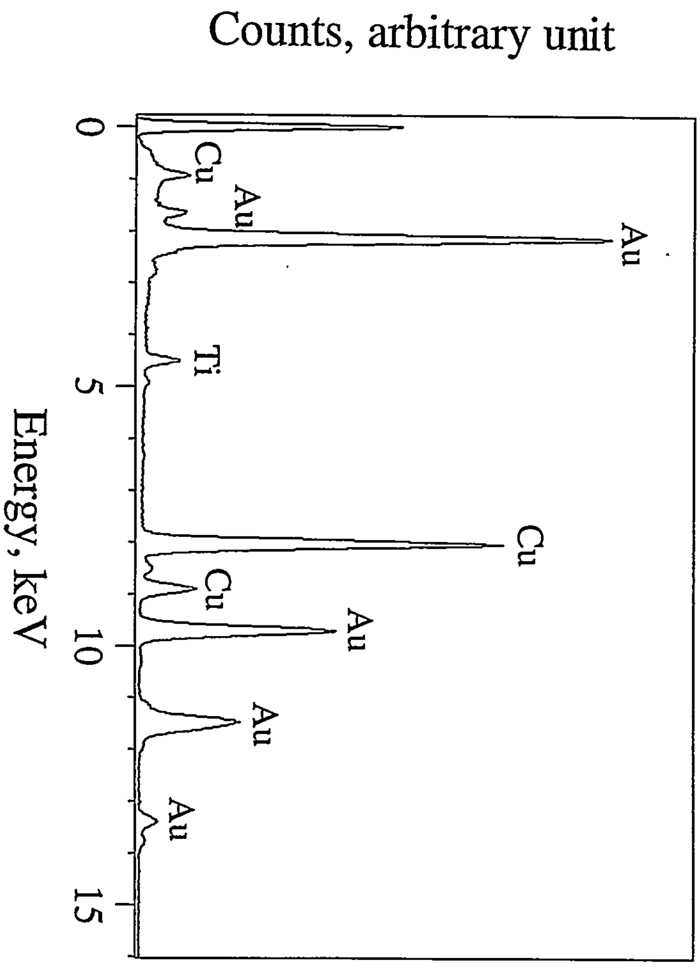
Counts, arbitrary unit
Energy, keV
0
5
10
15
Cu
Au
Au
Ti
Cu
Cu
Au
Au
Au

Fig. 7a

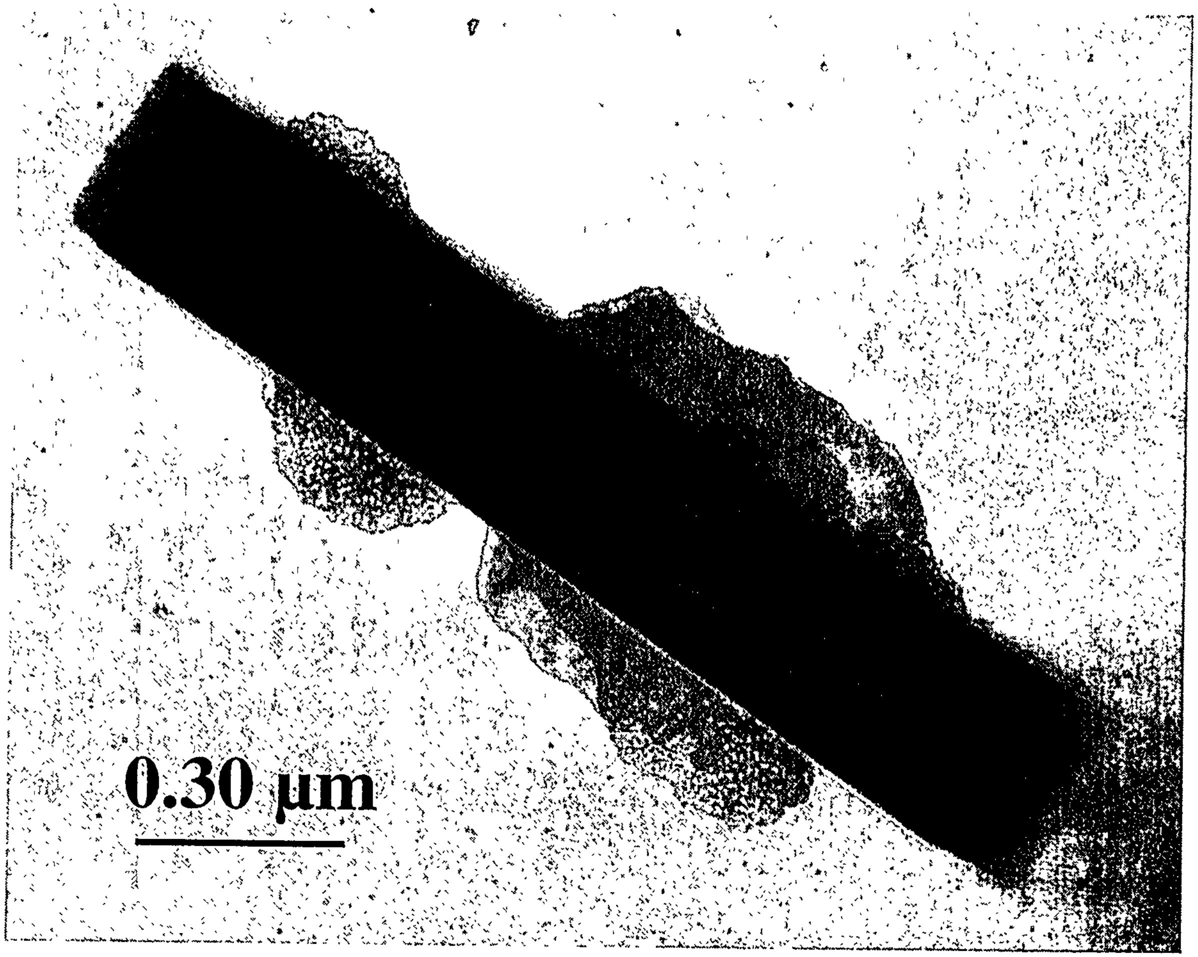

Fig. 76

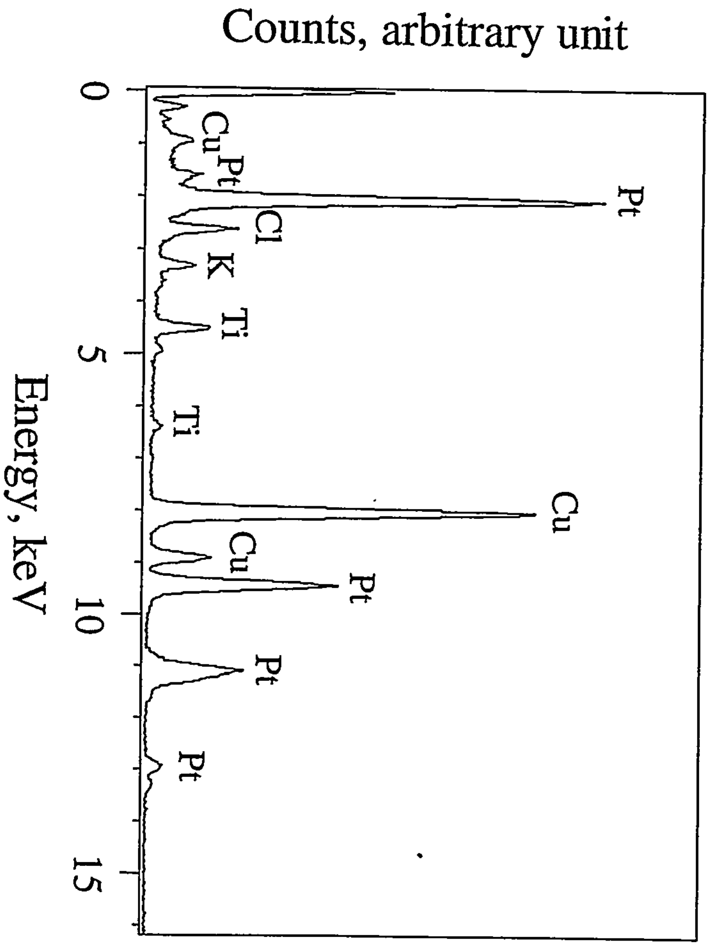

Counts, arbitrary unit
Energy, keV
0
5
10
15
Cu
Pt
Pt
Cl
K
Ti
Ti
Cu
Cu
Pt
Pt
Pt